NATURAL CIRCULATION OF ELECTRICALLY CONDUCTING LIQUIDS IN FUSION REACTOR BLANKETS

P.J. Gierszewski
B. Mikic
N.E. Todreas

PFC/JA 81-7

Submitted to Nuclear Engineering and Design
April 1981

Plasma Fusion Center
Fusion Blanket and Structures Group
Massachusetts Institute of Technology
Cambridge, MA 02139

NATURAL CIRCULATION OF ELECTRICALLY CONDUCTING LIQUIDS IN FUSION REACTOR BLANKETS

P.J. Gierszewski
B. Mikic
N.E. Todreas

Abstract

A simple model has been developed for heat transfer in fusion reactor blankets with liquid breeding regions, allowing for natural circulation and the presence of strong magnetic fields. The results have been compared with the limited information available.

For typical fusion blanket dimensions and temperature differences, natural circulation can be the dominant heat transfer mechanism in the molten salt flibe even over 10 Tesla magnetic field strength; it will increase heat transfer appreciably in the liquid lithium-lead mixture $Li_{17}Pb_{83}$ for magnetic field strengths less than about 10 Tesla; and can be neglected in liquid lithium if the magnetic field is over 1 Tesla.

Nomenclature

B	Magnetic field density, Tesla
C	Defined in Eqn.(21)
c_p	Specific heat at constant pressure, J/kg-K
E	Electric field strength, V/m
F	Body force, N/m^2
g	Acceleration due to gravity, 9.8 m/s^2
Gr	Grashof number, $Gr = g\beta L^3\rho^2\Delta T/\mu^2$
h	Heat transfer coefficient, W/m^2-K
Ha	Hartmann number, $Ha = BL\ (\sigma/\mu)^{0.5}$
J	Current density, A/m^2
k	Thermal conductivity. W/m-K
L	Length scale, m
Nu	Nusselt number, Nu = hL/k
p	Pressure, N/m^2
Pe	Peclet number, $Pe = PrRe = \rho c_p vL/k$
Pr	Prandtl number, $Pr = \mu c_p/k$
q"	Heat flux, W/m^2
Ra	Rayleigh number, Ra = GrPr
Ra_c	Critical Rayleigh number for onset of convection
Re	Reynolds number, $Re = \rho vL/\mu$
Re_m	Magnetic Reynolds number, $Re_m = \mu_m \sigma vL$
S	Magnetic force coefficient, $S = \sigma LB^2/\rho v$
T	Temperature, K
v	Fluid velocity, m/s
β	Thermal coefficient of volume expansion, 1/K
ΔT	Temperature difference, K
ρ	Fluid density, kg/m^3
$\bar{\rho}$	Average fluid density, kg/m^3
σ	Electrical conductivity, 1/ohm-m
μ	Viscosity, kg/m-s
μ_m	Magnetic permeability, approximately $4\pi x10^{-7}$ $V\text{-}s^2/C\text{-}m$

Subscripts

H,C	Hot, Cold
W,F	Wall, Fluid
BL,NC	Boundary Layer, Natural Circulation

NATURAL CIRCULATION OF ELECTRICALLY CONDUCTING LIQUIDS IN FUSION REACTOR BLANKETS

1. Introduction

Natural circulation in fusion reactor blankets containing liquid breeding regions (and liquid coolants) is of interest in normal operation, shutdown and accident states as a potential heat transfer mechanism [1,2]. Since the most promising liquid breeding materials (lithium, flibe and lithium-lead) are electrically conducting, the magnetic fields in many reactor concepts will inhibit this motion. In this paper, a simple model is developed for heat transfer in fusion reactor blankets, allowing for natural circulation and the presence of strong magnetic fields.

In the next sections, we review magnetic field effects, estimate natural circulation velocities through simple force balances with adjustments from some numerical analysis, calculate and compare Nusselt number heat transfer correlations for electrically conducting fluids in magnetic fields, and apply the results to fusion blanket conditions.

2. Magnetic Field Effects

This section is a brief discussion of magnetic field effects on a fluid. The basic assumptions are that the fluid is a continuum, that it is locally electrically neutral, and that there are no large relative motions of ions and electrons which could induce electric fields or make the transport coefficients anisotropic [3,4,5].

The electromagnetic field introduces four forces: the ponderomotive, electrostatic, magnetostrictive and electrostrictive forces. The ponderomotive force arises from current crossing magnetic field lines as

$$\underline{F} = \underline{J} \times \underline{B} \qquad (1)$$

where $\underline{F}$ is the force (N/m^2), $\underline{J}$ is the current density (A/m^2), and $\underline{B}$ is the magnetic field density (Tesla). The electrostatic force is the usual electric field - charged particle interaction. The magnetostrictive and electrostrictive forces arise from the elastic deformation of the fluid. They are related to the variation in field strength and, especially in uniform fields, to the variation in magnetic permeability and dielectric susceptibility. These are typically small forces, but not always negligible. For example, the electric forces may be important in free convection of polar liquids in strong electric fields - heat transfer from a heated wire inside a water-filled horizontal cylinder is increased by 50% if a strong electric field is applied between the wire and cylinder [3,4].

In the absence of an externally imposed current, currents can still exist in a moving fluid according to the more general form of Ohm's law

$$\underline{J} = \sigma(\underline{E}+\underline{v}\times\underline{B}) \qquad (2)$$

where σ is the fluid electrical conductivity (1/ohm-m), $\underline{E}$ is the electric field strength (volts/m) and $\underline{v}$ is the fluid velocity (m/s). This expression neglects anisotropic terms and Hall currents as is reasonable at liquid densities. This current can produce a significant ponderomotive force through Eqn. (1), and can itself create an electromagnetic field. The importance of these effects can be estimated by means of three dimensionless parameters; the magnetic force coefficient (S), the Hartmann number (Ha) and the magnetic Reynolds number (Re_m). These are defined as

$$S = \frac{\sigma B^2 L}{\rho v} = \frac{\text{ponderomotive force}}{\text{inertia force}} \tag{3}$$

$$Ha^2 = S\,Re = \frac{\sigma B^2 L^2}{\mu} = \frac{\text{ponderomotive force}}{\text{viscous force}} \tag{4}$$

$$Re_m = \frac{\mu_m J L}{B} = \mu_m \sigma v L = \frac{\text{induced magnetic field}}{\text{applied magnetic field}} \tag{5}$$

where ρ is the fluid density (kg/m^3), L is a characteristic length scale (eg. the radius of circular tube channel), Re is the usual Reynolds number, μ is the fluid viscosity (kg/m-s), and μ_m is the magnetic permeability ($\mu_m \sim 4\pi \times 10^{-7}$ V-s^2/C-m). In fusion reactor blankets, S and Ha can be greater than unity, and Re_m is usually small.

From conservation of charge, the steady-state current given by Ohm's law must close on itself, either in the fluid to produce local eddy currents, or through an external circuit. In forced convection flow through a conducting wall channel, the current can return through the walls, leaving a net decelerating force on the fluid. If the walls are insulated, the eddy currents may be forced back through the boundary layer, accelerating the flow there but resulting in little net force on the fluid since the center is decelerated. This produces a flattened "Hartmann" velocity profile. In more complex situations such as 3-D natural convection cells, the corresponding current paths may not be obvious and finding the self-consistent flow and current patterns may require solving a more complete set of magnetohydrodynamic equations.

The energy equation in the presence of a magnetic field can become quite complex. However, if magnetoelectrostriction is not important, the only significant addition is a simple joule heating term representing resistive dissipation of the current.

Some macroscopic consequences of these magnetic field effects are the suppression of turbulence and changes in the stability of natural circulation cells. In forced convection pipe flow, for example, the Reynold's number for transition to turbulent flow is raised to $Re \sim 500\,Ha$ where Ha is the Hartmann number for the transverse magnetic

field. The effect on natural circulation is not as easily quantified, and the following brief review is intended mainly to show trends. For a recent review of natural circulation in enclosures without magnetic fields, see Catton [6].

In the classical problem of density-driven convection between two infinite, rigid, horizontal plates with the lower one heated, the transition from static fluid to laminar 2-D rolls occurs at a critical Rayleigh number (Ra = Gr Pr) of $Ra_c \sim 1700$, to laminar 3-D cells around $Ra \sim 20000$, and to turbulent 3-D flow for Ra from 5×10^4 to 10^6 [7,8,9]. A magnetic field delays these transitions, for large fields, $Ra_c \sim Ha^2$ [10]. Adding vertical side walls also raises Ra_c, one study estimated this effect as $Ra_c \sim 1300\ L/V^{0.33}$ where L is the vertical height and V is the volume [11]. However, a compensating destabilizing factor in fusion blankets is that the heat source is internal. This could reduce Ra_c by as much as a factor of three based on the hot spot to wall temperature drop [12]. Even the size of the cells is affected by the magnetic field, one study suggesting a decrease with increasing field strength [10].

3. Natural Circulation Velocity

3.1 Order-of-magnitude estimate

Liquid breeding blanket designs remove heat by actively circulating the breeding material itself [13], or through a separate array of internal [14] or external [1] forced convection coolant tubes. In the latter cases, energy is deposited volumetrically by fusion neutrons and conducted through the breeding material to the coolant. Under the action of gravity (and depending on the orientation of the tubes), the resulting temperature distribution can give rise to natural circulation in the breeding material and enhance heat transfer.

However, as the previous section indicated, the presence of a strong magnetic field introduces new effects. For liquid lithium, flibe and $Li_{17}Pb_{83}$ in a fusion reactor blanket with steady, relatively uniform magnetic fields and no imposed currents or electric fields, the most significant new term is the ponderomotive force

$$\underline{F} = \underline{J} \times \underline{B} = \sigma(\underline{v} \times \underline{B}) \times \underline{B} \qquad (6)$$

The Navier-Stokes equations for an incompressible fluid (although small density variations will be included in the gravity body force) can be written as

$$\rho\left(\frac{\partial \underline{v}}{\partial t} + \underline{v}\cdot\nabla\underline{v}\right) = \underline{F} - \nabla p + \mu\nabla^2\underline{v} \qquad (7)$$

where, for fusion reactor blanket conditions, the general body force $\underline{F}$ is the local gravity force ($\rho\underline{g}$, where ρ is the local density) plus the ponderomotive force, Eqn. (6). If we assume steady-state ($\partial/\partial t = 0$) and approximate ∇p as the hydrostatic pressure gradient ($\bar{\rho}\underline{g}$, where $\bar{\rho}$ is the average density) then Eqn. (7) becomes

$$\rho\underline{v}\cdot\nabla\underline{v} = (\rho-\bar{\rho})\underline{g} + \sigma(\underline{v}\times\underline{B})\times\underline{B} + \mu\nabla^2\underline{v} \qquad (8)$$

In general, the solution of this momentum equation plus the mass and energy equations yields a three-dimensional flow pattern. However, to estimate the flow velocity we can simply use the force balance implied by Eqn. (8) to obtain the correct scaling. A plausible flow pattern is indicated in Figure 1, showing that the induced currents can close on themselves through conducting side walls or the side wall boundary

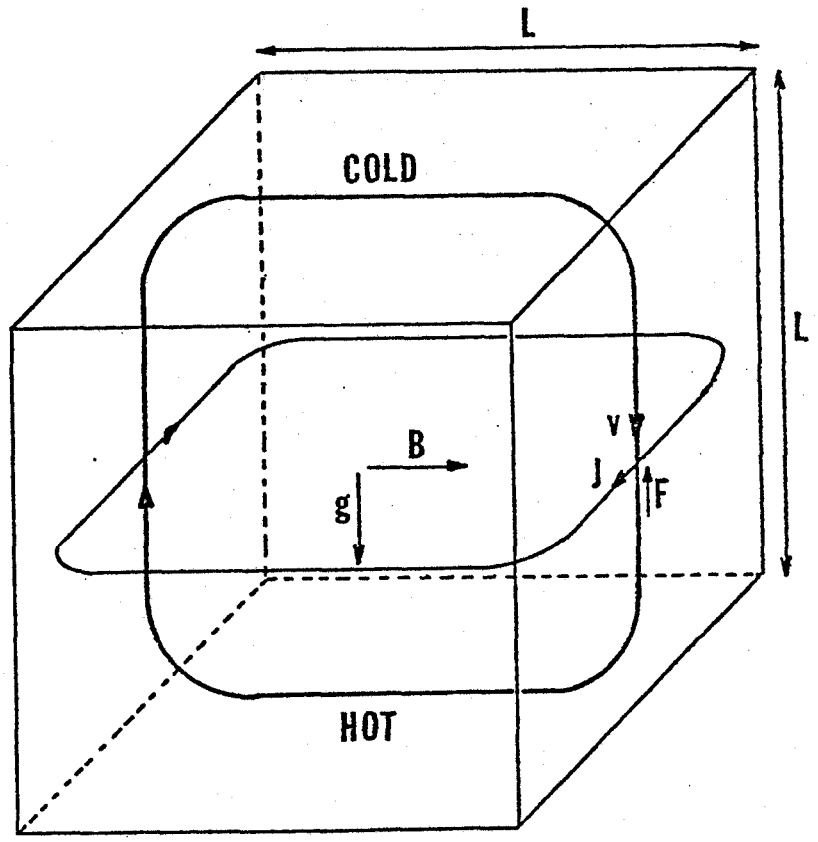

Figure 1. Possible circulation pattern showing induced current and ponderomotive force directions for a natural circulation cell in a magnetic field.

layers. Note that the two horizontal legs of the flow loop are parallel to the field so that they generate no current or force.

From Eqn. (8), the buoyancy force accelerating the flow is balanced by the inertial, ponderomotive and viscous forces. So, for an order-of-magnitude estimate,

$$\frac{\rho v^2}{L} \sim \rho\beta\Delta T g - \sigma v B^2 - \frac{\mu v}{L^2} \qquad (9)$$

where $\beta = \frac{-1}{\rho}\frac{\partial\rho}{\partial T} \sim \frac{-1}{\rho}\frac{\Delta\rho}{\Delta T}$ is the thermal coefficient of expansion;

ΔT is the driving temperature difference (between hot and cold regions);

L is a length scale (the distance between hot and cold regions).

Solving Eqn. (9) for the velocity,

$$v \sim \frac{L}{2}\left(\frac{\mu}{\rho L^2} + \frac{\sigma B^2}{\rho}\right)\left\{\left[1 + \frac{4g\beta\Delta T/L}{\left(\mu/\rho L^2 + \sigma B^2/\rho\right)^2}\right]^{1/2} - 1\right\} \qquad (10)$$

In practice, Eqn. (10) has two simple limits because of the fairly small viscosity of lithium, flibe and $Li_{17}Pb_{83}$ at reactor blanket conditions ($Gr > 10^6$ for cases studied here). For a small magnetic field, the steady-state velocity is just a balance between inertia and buoyancy, yielding

$$v \sim \sqrt{Lg\beta\Delta T} \qquad (11)$$

For large magnetic fields, the flow velocity is small so that the inertia term can be neglected, and the balance is between the buoyancy and the ponderomotive forces, yielding

$$v \sim \rho g\beta\Delta T/\sigma B^2 \qquad (12)$$

3.2 Numerical Analysis

The simple analysis presented above is expected to overestimate the flow velocity (and so the heat transfer) since it only considers the force balance in the buoyancy-driven section of the natural convection cell and ignores resistance to flow in the other sections. A numerical approach was investigated to account for full flow loop effects. In particular, the three-dimensional fission reactor thermal-hydraulics code THERMIT was modified to handle liquid lithium and liquid flibe blanket cooling in the presence of a steady, uniform magnetic field.

THERMIT existed for water and sodium coolants, and the new versions were obtained by adding the ponderomotive force to the liquid momentum equations and changing the fluid properties. The present water version of THERMIT is described in detail by Kelly and Kazimi [15], the sodium version by Wilson and Kazimi [16], and the lithium and flibe versions by Gierszewski et al [17]. The results of the code calculations are assumed applicable to the low Prandtl number liquid $Li_{17}Pb_{83}$.

The geometry used in the calculations is shown in Figure 2a. The blanket section was modelled with nine fluid mesh cells with a heat source in the bottom and a heat sink in the top middle cells, a situation which sets up an unstable density gradient. The sides, bottom and top side walls were adiabatic and impervious, while the top middle cell had a constant pressure boundary condition to allow for expansion. Viscous forces at these boundaries and within the fluid itself were neglected.

A steady-state circulation pattern is shown in Figure 2b. The four-cell pattern is a consequence of the source/sink placement in the large grid, 2-D system. More careful modelling could use the small grid, 3-D capabilities of the code, but the present approach provided a first order correction to Eqn. (10) to account for flow resistance around the full circulation cell.

3.3 Comparison of Velocity Estimates

The calculated velocities for sodium, lithium and flibe are given in Table 1. The input power is the total power flowing through the module from source to sink. For a given power, the steady-state temperature difference was calculated using THERMIT. ΔT is the driving temperature difference between the center cell and the source or sink cells, over a distance L. The THERMIT velocity is the flow velocity across this boundary. Average fluid properties are given in Table 2.

The calculated velocities show the expected behaviour of decreasing as the magnetic field increased or the temperature difference decreased.

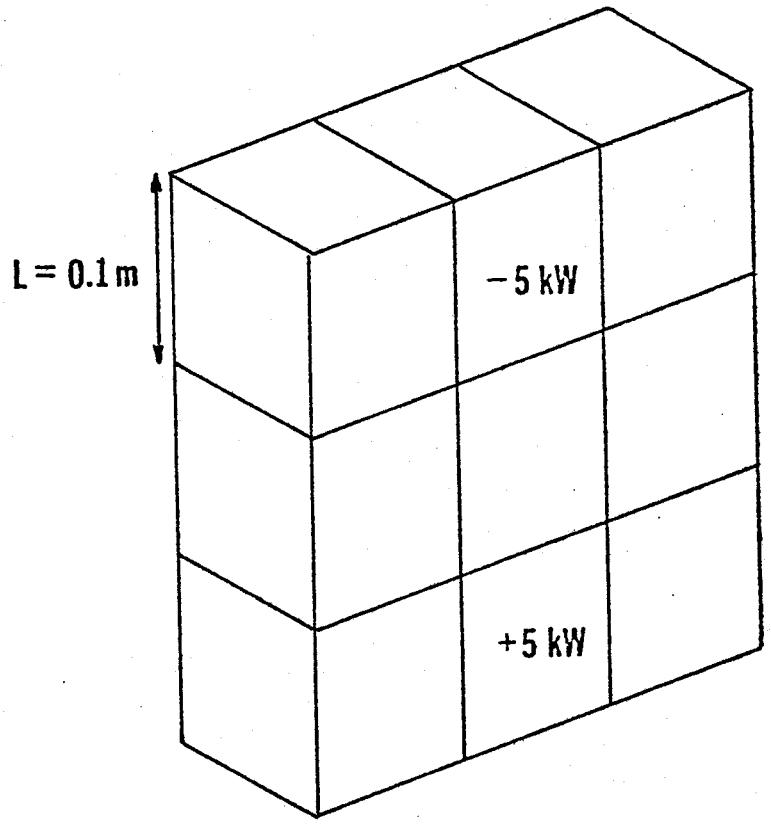

Figure 2.(a) Representative blanket module showing nine fluid mesh cells and source/sink placement.

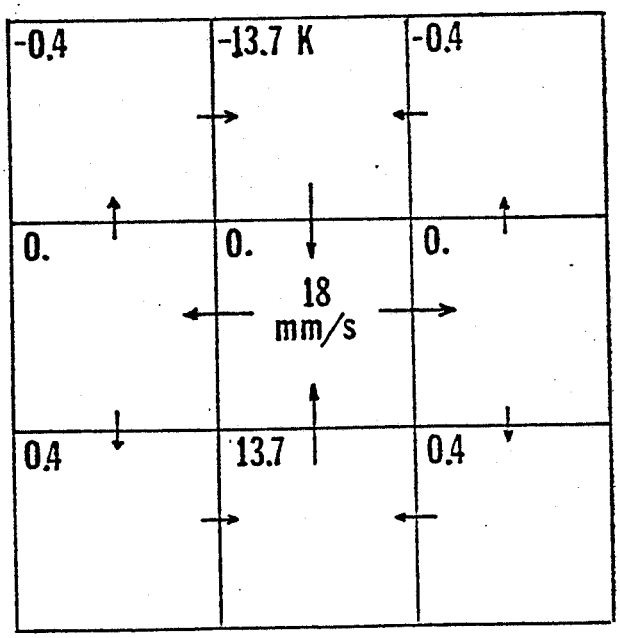

Figure 2.(b) Steady-state circulation pattern for lithium with no magnetic field, showing interface flow velocities (mm/s) as arrows and cell average temperature changes (K) in upper left corners.

Table 1. Calculated values of convection velocity

Magnetic field (T)	Input power (kW)	ΔT (K)	Convection velocity (mm/s) Eqn. (10)	THERMIT
Sodium (L = 0.1 m)				
0.	5.	19.	75.	23.
	0.5	4.3	36.	12.
0.1	5.	170.	14.	1.9
0.3	5.	270.	2.4	0.2
Lithium (L = 0.1 m)				
0.	5.	51.	100.	18.
	0.5	3.0	25.	8.5
	0.05	0.63	11.	3.8
0.1	5.	190.	7.1	0.6
	0.05	1.8	0.065	0.0064
0.3	5.	170.	0.70	0.07
	0.5	17.	0.072	0.007
Flibe (L = 0.1 m)				
0.	5.	7.6	39.	15.
0.1	5.	7.6	39.	15.
1.0	5.	9.8	39.	12.
10.	5.	69.	12.	1.3
	0.5	9.7	1.7	0.19
	0.05	1.0	0.17	0.02
20.	5.	93.	4.0	0.45
	0.5	10.	0.43	0.051
	0.05	1.	0.044	0.005
Flibe (L = 1.0 m)				
5.	500.	85.	58.	6.7
	5.	0.11	0.077	0.0085
10.	500.	11.	1.9	0.21
	50.	1.1	0.19	0.021

Table 2. Average fluid properties (900 K)*

Property	Lithium	Sodium	Flibe	$Li_{17}Pb_{83}$
k, W/m-K	52.	61.	1.0	22.
ρ, kg/m^3	472.	803.	1950.	9200.
μ, kg/m-s	2.7×10^{-4}	2.0×10^{-4}	7.5×10^{-3}	1.3×10^{-3}
c_p, J/kg-K	4190.	1250.	2350.	850.
σ, 1/ohm-m	2.6×10^{6}	2.9×10^{6}	230.	1.1×10^{6}
β, 1/K	2.1×10^{-4}	3.0×10^{-4}	2.1×10^{-4}	7.6×10^{-5}
Pr	0.022	0.0041	17.6	0.050
Gr/L^3 T, 1/m^3-K	6.3×10^{9}	4.7×10^{9}	1.4×10^{8}	3.7×10^{10}

*Lithium, sodium and flibe properties are from Gierszewski et al [18], some Li-Pb data from Sze et al [19] and the rest from linear interpolation in atom percent composition between lithium and lead properties.

Lithium and sodium were strongly affected at only one Tesla while flibe (because of its lower electrical conductivity) could tolerate twenty Tesla for the same reduction in flow velocity.

Comparing the convection velocities (Table 1), the order-of-magnitude estimates are higher by about a factor of three to nine. The simple analysis is expected to overestimate the flow velocity since, for example, it only considers the force balance in the buoyancy driven section of the natural circulation cell and ignores resistance to flow in the other sections. If we model this and any other effects by decreasing the buoyancy force in the driving section, then a reduction factor of about ten brings the two velocity calculations to within about 40% of each other.

A number of assumptions were made in both approaches regarding which electromagnetic effects could be neglected, and it is worthwhile to check these by calculating the dimensionless parameters S, Ha and Re_m, Eqn. (3) to (5). For the results given in Table 1, the magnetic force coefficient and the Hartmann number squared ranged over 0 to 10^8, indicating that the ponderomotive force varied from nonexistent to dominant with respect to inertial and viscous forces. The magnetic Reynolds number was always less than 0.01, so the neglect of induced magnetic fields was justified.

The flow Rayleigh numbers were all larger than 10^5 which should be well above the critical value for initiation of natural circulation. However, the convection pattern would probably not be simple, large 2-D rolls but more complicated, possibly turbulent, 3-D cells. Consequently the calculated heat convection probably overestimates the true heat transfer because of the large finite difference mesh size, but underestimates since flow was constrained to laminar 2-D motion rather than turbulent 3-D motion [6].

4. Natural Circulation Heat Transfer

In fusion blanket design, we are not interested in the circulation velocity per se, but rather in the heat transfer capabilities of the blanket if natural circulation is possible. In this section, we develop simple heat transfer models and compare them with the limited experimental data and other analysis.

First consider heat transfer across two plates with hot and cold wall temperatures T_{HW} and T_{CW}, separated by a liquid layer of thickness L. With pure conduction,

$$q'' = \frac{k}{L} (T_{HW} - T_{CW}) \tag{13}$$

For heat transfer by natural circulation, the enclosure is modelled as a circulation cell connecting boundary layers at the hot and cold walls (Figure 3). The fluid temperature at the two walls are T_{HF} and T_{CF} and are related to the heat flux by a boundary layer heat transfer coefficient h_{BL},

$$q'' = h_{BL} (T_{HW} - T_{HF}) = h_{BL} (T_{CF} - T_{CW}) \tag{14}$$

The internal heat transfer by convection is

$$q'' \sim \frac{\rho v c_p}{2} (T_{HF} - T_{CF}) \tag{15}$$

where $\rho v/2$ is the mass flux circulating in the convection loop. Combining Eqns. (14) and (15), heat transfer by natural circulation alone is

$$q'' = \frac{h_{BL}(\rho v c_p/2)}{h_{BL} + \rho v c_p} (T_{HW} - T_{CW}) \tag{16}$$

In practice, conduction and circulation can occur simultaneously. As a first approximation, treat these two mechanisms as independent, so

$$q'' \sim q''_{conduction} + q''_{convection} \sim \left[\frac{k}{L} + \frac{h_{BL}(\rho v c_p/2)}{h_{BL} + \rho v c_p}\right] (T_{HW} - T_{CW}) \tag{17}$$

Then the effective Nusselt number for heat transfer across the enclosure is

$$\overline{Nu} = \frac{Lq''/k}{(T_{HW} - T_{CW})} \sim 1 + \frac{Nu_{BL}(\rho v c_p L/2k)}{Nu_{BL} + (\rho v c_p L/k)} \tag{18}$$

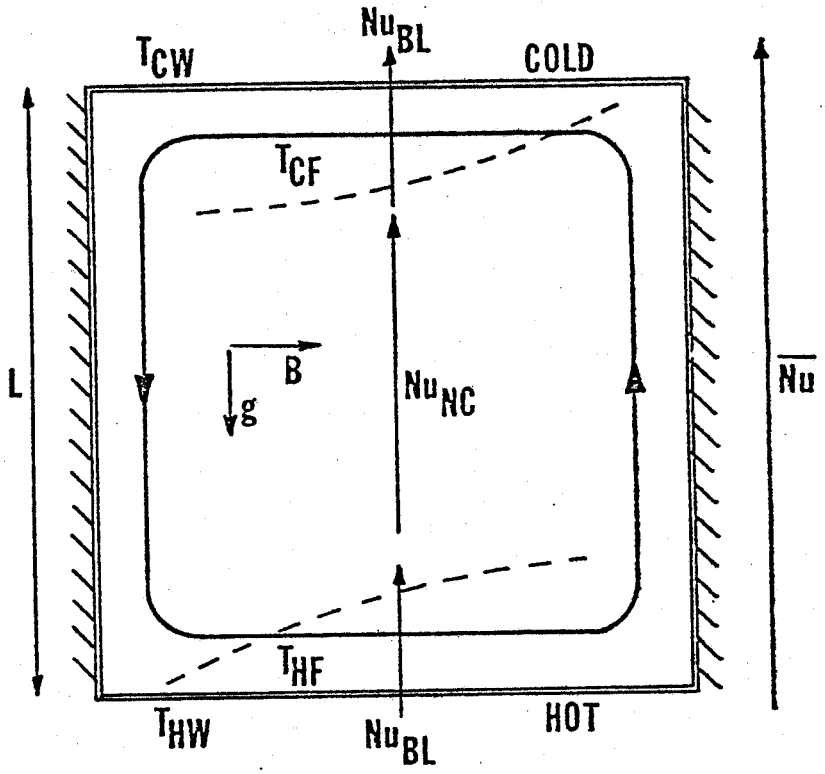

Figure 3. Model for heat transfer across two plates separated by a circulating liquid and adiabatic, non-conducting side walls.

where $Nu_{BL} = h_{BL}L/k$. Eqn. (18) reduces, as expected, to $\overline{Nu} = 1$ for pure conduction and to $\overline{Nu} \sim 0.5\ Nu_{BL}$ for natural circulation dominated by heat transfer resistance across the wall boundary layers.

Correlations are available for Nu_{BL} - for example, Gebhart [20] gives the following expressions for a laminar boundary layer along a plate,

$$Nu_{BL} \sim \begin{cases} 1.1\ Re^{0.5}\ Pr^{0.5} & Pr << 1 \\ 0.67\ Re^{0.5}\ Pr^{0.33} & Pr > 0.5 \end{cases} \tag{19}$$

For steady-state natural circulation, we approximate the boundary layer heat transfer by these correlations.

The internal natural circulation heat transfer is

$$\frac{\rho v c_p L}{k} \equiv \frac{Pe}{2} \tag{20}$$

where the Peclet number is also the ratio of convection heat transfer to conduction heat transfer.

Since $Pe = Pr\ Re$, Nu_{BL} can also be expressed as $Nu_{BL} = C\ Pe^{0.5}$ where $C \sim 1.1$ for $Pr << 1$ and $C \sim 0.67/Pr^{0.17}$ for $Pr > 0.5$. Thus the net heat transfer, Eqn. (18) is

$$\overline{Nu} \sim 1 + \frac{0.5\ Pe}{1 + Pe^{0.5}/C}; \qquad C = \begin{cases} 1.1 & Pr << 1 \\ 0.67/Pr^{0.17} & Pr > 0.5 \end{cases} \tag{21a}$$

where

$$Pe = \frac{Pr}{2}\,(1 + Ha^2)\left\{\left[1 + \frac{0.4\ Gr}{(1+Ha^2)^2}\right]^{0.5} - 1\right\} \tag{21b}$$

from Eqn. (10) with the correction factor as discussed under Section 3.3, Comparison of Velocity Estimates.

Eqn. (21) can be compared with other experimental results and theoretical calculations. Consider three limits of magnetic field strength relative to the buoyancy driving force: negligible magnetic field effects ($Ha << 1$); small magnetic field effects ($Ha >> 1$ but $Ha^4/Gr << 1$); and strong magnetic field effects ($Ha >> 1$ and $Ha^4/Gr >> 1$). Tables 3, 4 and 5 show the corresponding limits of Eqn. (21) along with similar limits obtained from analysis of available reports. The results of this study are seen to be in general agreement with the literature.

Table 3. Nusselt number for heat transfer across enclosures
(One wall heated, the other wall cooled)
Negligible magnetic field effects, Ha $\ll$ 1

$\overline{Nu}$		Comments	Reference
$Pr \ll 1$	$Pr \gtrsim 1$		
$0.3\ Gr^{0.25}\ Pr^{0.5}$	$0.2\ Gr^{0.25}\ Pr^{0.33}$	$H/W \sim 1$, $GrPr^2 \gg 1$	This study
	$0.07\ Gr^{0.33}\ Pr^{0.41}$	$Pr \sim 0.02$-3750, $Ra \sim 3\times10^5$-7×10^9	[20]
	$1.7\ Gr^{0.3}$	$H/W \sim 5$-10, $Pr \sim 1$, annular cavity$^+$	[21]
$Gr^{0.33}\ Pr^{0.66}$	$Gr^{0.33}\ Pr^{0.33}$	Ra large	[22]
	$0.1\ Gr^{0.29}\ Pr^{0.29}$	$H/W \sim 9$-36, $Gr \sim 4\times10^3$-3×10^5, 90°	[23]
	$0.1\ Gr^{0.29}\ Pr^{0.29}$	$H/W \sim 1$-3, $Ra \sim 4\times10^3$-10^7, oil and water$^+$	[24]
	$0.3\ Gr^{0.24}\ Pr^{0.24}$	$H/W \sim 4$-20, $Ra \sim 15\times10^4$-25×10^8, $Pr \sim 6^*$	[25]
$0.34(W/H)^{0.25}Gr^{.28}Pr^{.56}$	$0.22\ (W/H)^{0.25}(GrPr)^{0.28}$	$H/W \sim 2$-10, $Ra \sim 10^{10}$, $Pr \sim 10^5$, vertical	[6]
$0.58\ Gr^{0.25}\ Pr^{0.5}$	$0.55\ Gr^{0.25}\ Pr^{0.25}$	$H/W \sim 1$, $Pr \sim 0.02$, $Gr \sim 10^7$-10^8, vertical	[27]
$\dfrac{0.28\ (W/H)^{0.25}\ Gr^{0.25}\ Pr^{0.5}}{(Pr+0.95)^{0.25}}$		Vertical walls heated and cooled	[28]

Note: H is enclosure height, W is width;
Gr is based on distance between heated and cooled surfaces - H or W as appropriate
$^+$Correlations estimated *Internal heating

Table 4. Nusselt number for heat transfer across enclosures
(One wall heated, the other wall cooled)
Small magnetic field effects, $Ha \gg 1$ but $Ha^4/Gr \lesssim 1$

$\overline{Nu}/\overline{Nu}(Ha=0)$		Comments	Reference
$Pr \ll 1$	$Pr \gtrsim 1$		
$1 - 0.8\ Ha^2 / Gr^{0.5}$		H/W ~1, $GrPr^2 \gtrsim 10$	This study
$1 - 3\times10^4\ Ha/Gr$		$\underline{B} \parallel \underline{g}$, $Gr \sim 10^7$-10^9, $Pr \sim 0.02$, $Ha \sim$ 0-400	[27]
$1 - 0.3\ Ha^2/Gr^{0.5}$		Vertical plates heated and cooled+	[30]
$1 - 0.3\ Ha^2 / Gr^{0.5}\ (1+Pr)^{0.5}$		Vertical plates, $T_w - \bar{T} \sim x/L$	[28]
$1 - 0.36\ Ha^2/Gr^{0.5}$	$1 - 0.28\ Ha^2/Gr^{0.5}$	Vertical plates	[29]

Note: H is enclosure height, W is width;
Gr is based on distance between heated and cooled surfaces - H or W as appropriate

+Correlation estimated

Table 5. Nusselt number for heat transfer across enclosures
(One wall heated, the other wall cooled)
Strong magnetic field effects but appreciable convection
$Ha \gg 1$ and $Ha^4/Gr \gg 1$

$\overline{Nu}$		Comments	Reference
$Pr \ll 1$	$Pr \gtrsim 1$		
$0.2\ Pr^{0.5}\ Gr^{0.5}\ /\ Ha$	$0.1\ Pr^{0.33}\ Gr^{0.5}\ /\ Ha$	$H/W \sim 1$, $Gr \ll Ha^4 \lesssim (PrGr)^2$	This study
$0.5\ Pr^{0.5}\ Gr^{0.5}\ /\ Ha$		$Pr \sim 0.005$-0.01, $Ha/Gr^{0.25} \sim 5$-10, vertical plates, $\overline{Nu} \sim 0.5\ Nu_{plate}$	[26]
	$0.28\ Pr^{0.5}\ Gr^{0.5}\ /\ Ha$	Vertical plates, $T_w - \overline{T} \sim x/L$	[28]

Note: H is enclosure height, W is width.
Gr is based on distance between heated and cooled surfaces - H or W as appropriate

5. Heat Transfer in Fusion Blankets

In a tritium breeding fusion blanket, the heat source is internal volumetric heating while the heat sink may be a forced convection coolant passing through discrete tubes in the blanket. Thus the situation is not one of heat transfer between hot and cold walls, but between hot fluid in the blanket module interior and the nearby cold coolant tube walls. The heat transfer model, by analogy with Section 4, is natural circulation between a hot fluid region T_{HF} and a cold fluid layer near a wall T_{CF}, and then across the boundary layer to the cold wall at T_{CW}.

The overall Nusselt number for heat transfer from hot fluid to cooled wall is then

$$\overline{Nu} \sim 1 + \frac{Nu_{BL}(\rho v c_p L/2k)}{Nu_{BL} + (\rho v c_p L/2k)} = \frac{Pe/2}{1 + Pe^{0.5}/2C} \qquad (22)$$

where Pe and C are given in Eqn. (21).

Taking representative fluid properties from Table 2, Eqn. (22) is evaluated as a function of ΔT and B and the results are shown in Figure 4 for L = 0.1 m. $\overline{Nu}$ increases roughly as $\sqrt{L}$ so since L is unlikely to be much larger than 1 m, the potential heat transfer improvement is no more than about a factor of three.

The results show that natural circulation can be neglected in lithium regions with B > 1 T, can increase heat transfer appreciably even for B ~ 1 T in $Li_{17}Pb_{83}$, and is the dominant heat transfer mechanism in flibe even over 10 T. (Note that the onset of convection can be roughly estimated as $Ra_c \sim Ha^2$ for large Ha.)

Natural circulation has generally not been treated in detail in fusion reactor studies. It is therefore interesting to use the present results to evaluate two studies that did consider natural circulation. In Werner's lithium cassette blanket [1], the dimensions were chosen partly so as to prevent natural circulation from depositing hot center fluid on the coolant walls and possibly causing cyclic fatique problems.

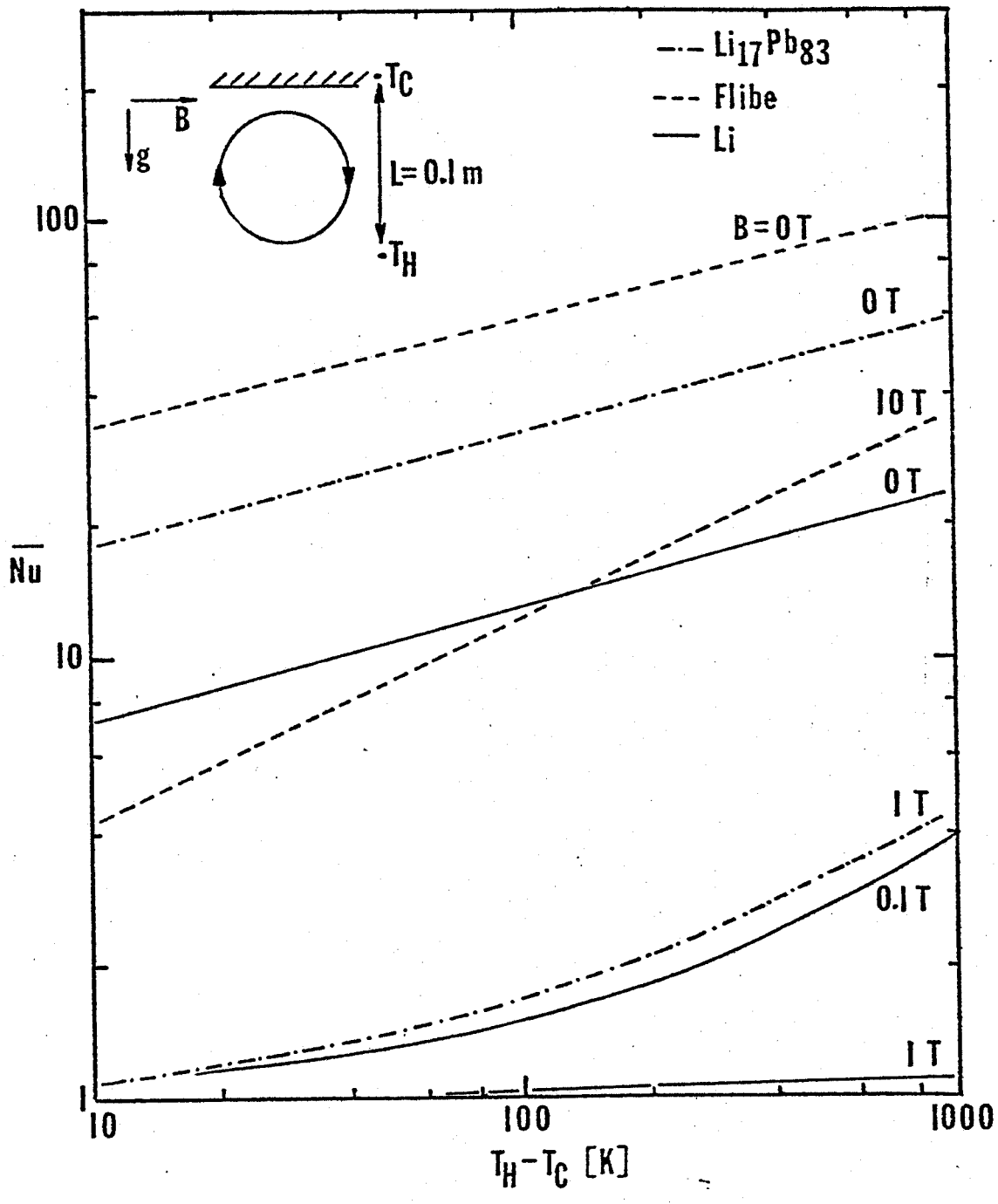

Figure 4. Nusselt number for heat transfer from hot interior fluid to cold surface with $Li_{17}Pb_{83}$, flibe or lithium under typical fusion blanket conditions. These curves are from Eqn. (22).

For $L \sim 0.03$ m, $\Delta T \sim 100$ K and $B \sim 1$ T, Eqn. (22) confirms that no circulation is expected. However in the TCT Hybrid blanket proposed by Aase et al [2], the flibe containing regions were expected to have substantial circulation. For $L \sim 0.1$ m, $\Delta T \sim 1000$ K, and $B < 5$ T, we indeed expect $\overline{Nu} \gg 1$ with circulation velocities on the order of 0.1 m/s.

6. Conclusions

A simple model has been developed for heat transfer in fusion blankets including natural circulation in the presence of strong magnetic fields. The results compare reasonably with the limited experimental data and other analyses described in the literature.

For typical fusion blanket dimensions and temperature differences, we conclude that natural circulation can be the dominant heat transfer mechanism in flibe even up to 10 Tesla magnetic field density, will increase heat transfer appreciably even around 1 Tesla in liquid $Li_{17}Pb_{83}$, but can be neglected in lithium regions with over 1 Tesla magnetic fields.

References

1. R. Werner, 'ORNL Fusion Power Demonstration Study: The Concept of the Cassette Blanket', Oak Ridge National Lab, ORNL/TM-5964, October 1977.

2. D.T. Aase et al, 'TCT Hybrid Preconceptual Blanket Design Studies', Battelle Pacific Northwest Labs, PNL-2304, January 1978.

3. M.F. Romig, 'The Influence of Electric and Magnetic Fields on Heat Transfer to Electrically Conducting Fluids', Advances in Heat Transfer (J.P. Hartnett and T.F. Irvine, eds.), Vol.1, Academic Press, Inc., New York, 1964.

4. M.F. Romig, 'Electric and Magnetic Fields', Handbook of Heat Transfer (W.M. Rohsenow and J.P. Hartnett, eds.), McGraw-Hill Co., New York, 1973.

5. M.A. Hoffman and G.A. Carlson, 'Calculational Techniques for Estimating the Pressure Losses for Conducting Fluid Flows in Magnetic Fields', Lawrence Radiation Laboratory, UCRL-51010, 1971.

6. I. Catton, 'Natural Circulation in Enclosures', Proceedings of the Sixth International Heat Transfer Conference, Toronto, Canada, August, 1978, Vol. 6, Keynote Papers, pp. 13-31.

7. Y. Nakagawa, 'Heat Transport by Convection in Presence of an Impressed Magnetic Field', Physics of Fluids, Vol. 3, 1960, pp. 87-93.

8. D.B. Thomas and A.A. Townsend, 'Turbulent Convection over a Heated Horizontal Surface', Journal of Fluid Mechanics, Vol. 2, 1957, pp. 473-492.

9. N.F. Veltishchev and A.A. Zelnin, 'Numerical Simulation of Cellular Convection in Air', Journal of Fluid Mechanics, Vol. 68, 1975, pp. 353-368.

10. U.H. Kurzweg, 'Convective Instability of a Hydromagnetic Fluid within a Rectangular Cavity', International Journal of Heat and Mass Transfer, Vol. 8, 1965, pp. 35-41.

11. W.L. Heitz and W.W. Westwater, 'Critical Rayleigh Numbers for Natural Convection of Water Confined in Square Cells with L/D from 0.5 to 8', ASME Journal of Heat Transfer, Vol. 93, 1971, pp. 188-196.

12. E.M. Sparrow, R.J. Goldstein and V.K. Jonsson, 'Thermal Instability in a Horizontal Fluid Layer: Effect of Boundary Conditions and Non-linear Temperature Profile', Journal of Fluid Mechanics, Vol. 18, 1964, pp. 513-528.

13. B. Badger et al, 'UWMAK-I, A Wisconsin Toroidal Fusion Reactor Design', UWFDM-68, University of Wisconsin, 1974.

14. R.G. Mills (ed.), 'A Fusion Power Plant', Princeton University, MATT-1050, 1974.

15. J.E. Kelly and M.S. Kazimi, 'Development and Testing of the Three-Dimensional, Two-Fluid Code THERMIT for LWR Core and Subchannel Applications', Massachusetts Institute of Technology Energy Lab Report, MIT-EL-79-046, December 1979.

16. G. Wilson and M.S. Kazimi, 'Development of Models for the Sodium Version of the Two-Phase Three-Dimensional Thermal Hydraulics Code THERMIT', M.I.T. Energy Lab Report, MIT-EL-80-010, May 1980.

17. P.J. Gierszewski, B. Mikic and N.E. Todreas, 'THERLIT and THERFLIBE, Thermal-Hydraulic Codes for Lithium and Flibe in a Magnetic Field', M.I.T. Nuclear Engineering Department, unpublished report, August 1979.

18. P.J. Gierszewski, B. Mikic and N.E. Todreas, 'Property Correlations for Lithium, Sodium, Helium, Flibe and Water in Fusion Reactor Applications', M.I.T. Plasma Fusion Center, PFC-RR-80-12, August 1980.

19. D.K. Sze, R. Clemmer and E.T. Cheng, 'LiPb, A Novel Material for Fusion Applications', University of Wisconsin, UWFDM-378, October 1980.

20. B. Gebhart, Heat Transfer, 2nd ed., McGraw-Hill Book Co., New York, 1971, pp. 241-245, 377.

21. 'Numerical Simulation of Natural Convection in Closed Containers by a Fully Implicit Method', Journal of Fluids Engineering, 99, December 1977, p. 649.

22. R.R. Long, 'Relation between Nusselt number and Rayleigh Number in Turbulent, Thermal Convection', Journal of Fluid Mechanics, 73, February 1976, p.445.

23. K.R. Randall, J.W. Mitchell, and M.M. El-Wakil, 'Natural Convection Heat Transfer Characteristics of Flat Plate Enclosures', Journal of Heat Transfer, 101, February 1979. p. 120.

24. J.N. Arnold, I. Catton and D.K. Edwards, 'Experimental Investigation of Natural Convection in Inclined Rectangular Regions of Differing Aspect Ratio', Journal of Heat Transfer, 98, February 1976, p.67.

25. F.A. Kulacki and M.E. Nagle, 'Natural Convection in a Horizontal Fluid Layer with Volumetric Energy Sources', Journal of Heat Transfer, 97, May 1975, p. 204.

26. K. Cramer, 'Several Magnetohydrodynamic Free-Convection Solutions', Journal of Heat Transfer, 85, 1963, p.35.

27. M. Seki, H. Kawamura and K. Sanokawa, 'Natural Convection of Mercury in a Magnetic Field Parallel to Gravity', Journal of Heat Transfer, 101, May 1979, p. 227.

28. A. Emery, 'The Effect of a Magnetic Field Upon the Free Convection of a Conducting Fluid', Journal of Heat Transfer, 85, 1963, p. 119.

29. E. Sparrow and R. Cess, 'The Effect of a Magnetic Field on Free Convection Heat Transfer', International Journal of Heat and Mass Transfer, 3, 1961, p.267.

30. D. Papailiou and P. Lykoudis, 'Magneto-fluid-mechanics Free Convection Turbulent Flow', International Journal of Heat and Mass Transfer, 17, 1974, p.1181.

Acknowledgements

This work originated under U.S. D.O.E. contract EY-76-S-02-2431. One of the authors, P. Gierszewski, was partially supported by a Canadian government postgraduate scholarship.